ISAR Echoes Coherent Processing and Imaging[1,2]

Xing Mengdao, LAN Jinqiao, BAO Zheng, Liao Guisheng
Key Laboratory of Radar Signal Processing
PO 374 Box, Key Laboratory for Radar Signal Processing,
Xidian University, Xi'an, Shaanxi, 710071, People's Republic of China
86-29-8202348
xmd@xidian.edu.cn

Abstract—The general approach to ISAR imaging is range-Doppler (RD) imaging approach. For this approach, the translational motion compensation (TMC) is firstly obtained by envelope alignment and autofocus, so the target can be treated as a rotating target for the next processing. But in this method, scatterers' migration through resolution cells (MTRC) caused by rotational motion is neglected. However in practice, MTRC exists with the improvement of resolution or for big target. For MTRC compensation, a keystone transformation in SAR is used in this paper. Before keystone transformation, it is demanded that the raw data is coherent, while in fact, the ISAR raw data is usually not. So a coherent processing of raw data is proposed. In this paper, the coherent processing of raw data is firstly done and the next step is to correct MTRC. Finally a parameter estimation method of multi-component amplitude modulation and linear frequency modulation (AM-LFM) signal is proposed to estimate the scatterers' instantaneous amplitudes and frequencies, and the Range-Instantaneous Doppler (RID) ISAR image is obtained. The effective of this algorithm is testified by the processing of simulation data.

TABLE OF CONTENTS

1. INTRODUCTION

Inverse synthetic aperture radar (ISAR) imaging has received intensive attention during the past twenty years [1-32], due to its capability to produce high-resolution target images over long ranges, under all weather conditions, day and night. Fine range resolution is obtain by transmitting a signal that has a wide frequency bandwidth. Doppler frequecny resolution, and hence crossrange resolution, inversely proportional to the coherent integration time interval/angle [1].

In ISAR, the relative motion needed to obtain the synthetic aperture is induced by the moving of target itself. In general, the relative radar/target motion can be decomposed into translational motion and rotational motion with respect to a reference point of the target. In order to obtain high resolution ISAR imaging, the translational motion must firstly be accurately compensated.

The translational motion compensation can usually be divided into two steps: envelope alignment and autofocus. There are a number of envelope alignment methods, such as, amplitude correlation method [2], improved correlation method called averaged correlation method [3], global range alignment method [4], and so on. There are also a large number of autofocus methods, such as, dominant scatterer algorithm [5], maximum-likelihood algorithm [6], centroid tracking algorithm [7], multiple PPP algorithm [8], PGA [9], contrast optimization algorithm [10], weighted least square algorithm [11], entropy minimization algorithm [12], AUTOCLEAN algorithm [31], and so on.

After the translational motion is compensated, the target can be treated as a rotating target with respect to a reference point. The rotation of an ISAR target can roughly be categorized into the following three classes [13]: (1) uniform planar rotation with a constant angular velocity, (2)

[1] 0-7803-8155-6/04/$17.00 © 2004 IEEE
[2] IEEEAC paper #1041, Version 3, Updated September 30, 2003

0-7803-8155-6/04/$17.00 ©2004 IEEE

nonuniform planar rotation with a time variant angular velocity, and (3) three dimensional (3-D) rotation with pitch, roll and yaw. For class (1), the range- Doppler (RD) algorithm or polar formation algorithm, can be used to form a focused ISAR image [1, 2]. For class (2), interpolation or time-frequency techniques can be used to form a focused ISAR image [13, 14]. For class (3), if the target is small, or the required resolution is low, the scatterers' migration through resolution cells (MTRC) caused by rotational motion can be ignored after range compression. The Doppler frequency of each scatterer is time-varying because the maneuvering target's rotational velocity and axis vary with time. In this case, the time-frequency analysis is used to obtain Range- Instantaneous Doppler (RID) images, and imaging problem became an instantaneous Doppler parameter estimation problem. A number of estimation methods or imaging methods have been proposed, such as, joint time-frequency method [15, 16], Radon-Wigner method [17], chirplet decomposition method [18], Extended Weighted RELAX method [13], Capon estimator method [19], smoothed-pseudo-Wigner-Ville (SPWV) transform method [20], 2-D ESPRIT method [25], short time Fourier transform method [26], and so on.

If the target is big, such as big airplane, ship, or the required resolution is very high such as 0.15m, the scatterers' MTRC caused by rotational motion can not be ignored. In this situation, the target's wavenumber support region can not be approximated as a rectangular plane or box, the wavenumber vectors with different spatial angles are not parallel to each other, so range curvature does occur. Because the rotation of a non-cooperative maneuvering target is usually nonuniform and three-dimensional (pitch, roll and yaw), moreover, the rotation is unknown and difficult to estimate, the polar formation algorithm is not suitable to overcome range curvature or MTRC caused by rotational motion.

In SAR, R.P Perry and Soumekh et al [21-23] proposed keystone transformation in the fast frequency-slow time domain, which can correct moving target's linear range migration caused by its linear constant velocity. In this paper this keystone transformation is used in ISAR to correct range movement (also called linear range migration, linear MTRC) caused by target's rotational motion, but keystone transformation is done in the fast time after range dechirping-slow time domain.

Before keystone transformation, it is demanded that the rawdata is coherent, while in fact, the ISAR rawdata is usually not because it is difficult to tracking the target center precisely. So a coherent processing of rawdata is proposed. In this paper, the rawdata is phase compensated in time domain and frequency domain to make it coherent. That is to say, on the basis of the general ISAR translational motion compensation which only the envelope alignment of rang image and the autofocus are done, the data are multiplied by the linear phase in rang image domain to make the envelope of rawdata also align. After this coherent processing the rawdata is completely coherent. In the next, the keystone transformation is done to correct linear MTRC.

After range movement correction and range compression, a parameter estimation method of multi-component amplitude modulation and linear frequency modulation (AM-LFM) signal is proposed to estimate the scatterers' instantaneous amplitudes and frequencies, and the RID ISAR image is obtained. The effective of this algorithm is testified by the processing of simulation data.

For the more, an analysis of velocity compensation of missile with high speed before coherent processing and a fast realization of keystone transformation are made. The one-dimension range image compensation can be done by phase compensation in time and frequency domains after the target's velocity has been estimated with map drift (MD) method commonly used in SAR autofocus. For keystone transformation, the fast realization is obtained by discrete Fourier transform and inverse fast Fourier transform (DFT-IFFT), or scaled Fourier transform and inverse fast Fourier transform (SFT-IFFT).

The remainder of this paper is outlined as follows. In Section II, the method for the coherent processing of ISAR echoes is investigated. In Section III, the scatterers' range movement correction is discussed. In Section IV, the azimuth imaging is presented. The whole algorithm block diagram is shown in Section V. The experimental results obtained by using simulation radar data are presented in Section VI. Finally in Section VII, the conclusion is given. In Appendix A, the preprocessing of the echoes of missile with high speed is analyzed, and in Appendix B, the fast realization of keystone transformation is introduced.

2. The Coherent Processing of ISAR Echoes

In theory, the coherent echoes of ISAR can be obtained by coherent receiver. In practice, in order to increase transmit power, and decrease the receiver bandwidth, the radar usually transmits LFM signal, and then dechirps the received signal. Suppose the transmitting signal is

$$s(\hat{t},t_m)=\mathrm{rect}\left(\frac{\hat{t}}{T_p}\right)\exp\left[j2\pi(f_c t+\frac{1}{2}\gamma\hat{t}^2\right], \quad (1)$$

where $\mathrm{rect}(u)=\begin{cases}1 & |u|\le\frac{1}{2}\\ 0 & |u|>\frac{1}{2}\end{cases}$, f_c is center frequency, T_p is pulse width, γ is the frequency modulation rate, $\hat{t}=t-mT$ is fast time. m is an integral number, T is pulse repetition period, $t_m=mT$ is slow time.

Suppose the target have Q scatterers, the range of i th scatterer from radar is $R_i(t_m)$, the received data is $s_R(\hat{t},t_m)$,

$$s_R(\hat{t},t_m)=\sum_i^Q A_i\mathrm{rect}\left(\frac{\hat{t}-2R_i(t_m)/c}{T_p}\right)e^{j2\pi\left(f_c\left(t-\frac{2R_i(t_m)}{c}\right)+\frac{1}{2}\gamma\left(t-\frac{2R_i(t_m)}{c}\right)^2\right)} \quad (2)$$

where c is the velocity of light. Because the echoes of every scatterers are independent, so the echoes $s_{iR}(\hat{t},t_m)$ of i th scatterer is firstly to be studied, that is

$$s_{iR}(\hat{t},t_m)=A_i\mathrm{rect}\left(\frac{\hat{t}-2R_i(t_m)/c}{T_p}\right)e^{j2\pi\left(f_c\left(t-\frac{2R_i(t_m)}{c}\right)+\frac{1}{2}\gamma\left(t-\frac{2R_i(t_m)}{c}\right)^2\right)} \quad (3)$$

where the range of this i th scatterer from radar is $R_i(t_m)$.

The reference range of the receiver dechirp signal is got by measuring range with low resolution echoed signal, so its error is large. Suppose range measured is $R_s(t_m)$, then the reference signal is

$$s_{ref}(\hat{t},t_m;R_s(t_m))=e^{j2\pi\left(f_c\left(t-\frac{2R_s(t_m))}{c}\right)+\frac{1}{2}\gamma\left(t-\frac{2R_s(t_m)}{c}\right)^2\right)}. \quad (4)$$

After dechirping,

$$\begin{aligned}s_i(\hat{t},t_m)&=s_{iR}(\hat{t},t_m)\cdot s_{ref}^*(\hat{t},t_m;R_s(t_m))\\&=A_i\mathrm{rect}\left(\frac{\hat{t}-2R_i(t_m)/c}{T_p}\right)\cdot e^{j\pi\gamma\left(\left(\frac{2R_i(t_m)}{c}\right)^2-\left(\frac{2R_s(t_m)}{c}\right)^2\right)}\\&\quad\cdot e^{-j2\pi\left(\gamma\left(\frac{2R_i(t_m)}{c}-\frac{2R_s(t_m)}{c}\right)\hat{t}+f_c\left(\frac{2R_i(t_m)}{c}-\frac{2R_s(t_m)}{c}\right)\right)},\end{aligned} \quad (5)$$

that is,

$$\begin{aligned}s_i(\hat{t},t_m)&=A_i\mathrm{rect}\left(\frac{\hat{t}-2R_i(t_m)/c}{T_p}\right)\\&\quad\cdot e^{-j\frac{4\pi}{c}\left(f_c+\gamma\left(\hat{t}-\frac{2R_s(t_m)}{c}\right)\right)(R_i(t_m)-R_s(t_m))}\,e^{j\frac{4\pi\gamma}{c^2}(R_i(t_m)-R_s(t_m))^2}.\end{aligned} \quad (6)$$

From Eq.(6) above, the received differential frequency is single and its value is proportional to the position of the scatterer. So, the complicated target's echoes are just the range images that take frequency as its parameter. If the reference range $R_s(t_m)$ is very close to the target, the bandwidth of the received differential frequency signal can be narrow. But From Eq.(6) above, because of the large error of the target range $R_s(t_m)$, moreover, the error is random, so the raw received signal is not coherent.

The movement of ISAR target can be decomposed into translational motion and rotational motion. It is needed to compensate the translational motion firstly and the target can be treated as a rotating target with respect to a reference center point. Suppose there is a virtual center point of the target O, its distance from the radar at time t_m is $R_O(t_m)$. In the following, a discussion of how to compensate the received data to make it to be a rotating model is made.

In the translational motion compensation, it is generally divided into two steps in practice, which are envelope alignment and the initial phase correction. For the phase correction, it is demanded that the phase error be smaller than $\pi/8$ that is corresponding to sub-millimeter, which is difficult to achieve in practice. But the influence of phase error is a value modulo 2π, so the initial phase correction is sufficient. For envelope alignment, it should be done with actual time, but the demanded precision is low, so in this paper, two-step compensations are made.

Suppose the reference range of the dechirping signal is $R_s(t_m)$, it is needed to compensate to virtual reference range $R_o(t_m)$ for dechirping, so a phase compensation function H_1 is constructed as

$$\begin{aligned}H_1(\hat{t},t_m)&=s_{ref}(\hat{t},t_m;R_s(t_m))\cdot s_{ref}^*(\hat{t},t_m;R_o(t_m))\\&=e^{j2\pi\left(f_c\left(t-\frac{2R_s(t_m))}{c}\right)+\frac{1}{2}\gamma\left(t-\frac{2R_s(t_m)}{c}\right)^2\right)}\\&\quad\cdot e^{-j2\pi\left(f_c\left(t-\frac{2R_O(t_m))}{c}\right)+\frac{1}{2}\gamma\left(t-\frac{2R_O(t_m)}{c}\right)^2\right)}.\end{aligned} \quad (7)$$

Let $\hat{t}_s=\hat{t}-\frac{2R_s(t_m)}{c}$, the signal's sampling region is $[-\frac{T_p}{2},\frac{T_p}{2}]$, and $R_{\Delta so}(t_m)=R_s(t_m)-R_o(t_m)$, Eq.(7) can be transformed to

$$H_1(\hat{t},t_m)=\exp\left\{-j\frac{4\pi}{c}(f_c+\gamma\hat{t}_s)R_{\Delta so}(t_m)-j\frac{4\pi\gamma}{c^2}(R_{\Delta so}(t_m))^2\right\}. \quad (8)$$

After multiplying received signal by H_1, the signal of the i th scatterer that has been phase compensated is

$$\begin{aligned}s_i(\hat{t},t_m)&=s_i(\hat{t},t_m)H_1(\hat{t},t_m)\\&=A_i\mathrm{rect}\left(\frac{\hat{t}-2R_i(t_m)/c}{T_p}\right)e^{-j\frac{4\pi}{c}\left(f_c+\gamma\left(\hat{t}-\frac{2R_s(t_m)}{c}\right)\right)(R_i(t_m)-R_o(t_m))}\\&\quad\cdot e^{j\frac{4\pi\gamma}{c^2}[(R_i(t_m)-R_s(t_m))^2-(R_s(t_m)-R_o(t_m))^2]},\\&=A_i\mathrm{rect}\left(\frac{\hat{t}-2R_i(t_m)/c}{T_p}\right)e^{-j\frac{4\pi}{c}\left(f_c+\gamma\left(\hat{t}-\frac{2R_s(t_m)}{c}\right)\right)(R_i(t_m)-R_o(t_m))}\\&\quad\cdot e^{j\frac{4\pi\gamma}{c^2}\left\{[R_i(t_m)-R_o(t_m)]^2-2[R_i(t_m)-R_o(t_m)][R_s(t_m)-R_o(t_m)]\right\}}\end{aligned} \quad (9)$$

which can be simplified as

$$\begin{aligned}s_i(\hat{t},t_m)=s_i(\hat{t},t_m)H_1(\hat{t},t_m)&=A_i\mathrm{rect}\left(\frac{\hat{t}-2R_i(t_m)/c}{T_p}\right)\cdot\\&e^{-j\frac{4\pi}{c}\left(f_c+\gamma\left(\hat{t}-\frac{2R_O(t_m)}{c}\right)\right)(R_i(t_m)-R_o(t_m))}\,e^{j\frac{4\pi\gamma}{c^2}(R_i(t_m)-R_o(t_m))^2}.\end{aligned} \quad (10)$$

After the compensation of $H_1(\hat{t},t_m)$, the phase of signal has been compensated to be dechirping form where reference range is $R_o(t_m)$. But the sampling region still exists error because of the difference between $R_o(t_m)$ and $R_s(t_m)$, so it needs to compensate. The envelope movement compensation can be achieved in frequency domain where the second phase term in Eq.(10) that is residual video phase (RVP) can be compensated at the same time. In the following, Fourier transform with respect to $\hat{t}_s$ results in [8]

$$S_i(f_i,t_m)=A_iT_p\mathrm{sinc}\left(T_p(f_i+2\frac{\gamma}{c}(R_i(t_m)-R_o(t_m))\right)\cdot e^{-j\frac{4\pi}{c}\left(f_c+\gamma(\frac{2R_i(t_m)}{c}-\frac{2R_o(t_m)}{c})\right)(R_i(t_m)-R_o(t_m))}\cdot e^{j\frac{4\pi\gamma}{c^2}(R_i(t_m)-R_o(t_m))^2}\cdot e^{-j2\pi f_i\left(\frac{2R_i(t_m)}{c}-\frac{2R_s(t_m)}{c}\right)}, \quad (11)$$

which can be simplified as

$$S_i(f_i,t_m)=A_iT_p\mathrm{sinc}\left(T_p(f_i+2\frac{\gamma}{c}(R_i(t_m)-R_o(t_m))\right)\cdot e^{-j\frac{4\pi}{c}f_c(R_i(t_m)-R_o(t_m))}\cdot e^{-j\frac{4\pi\gamma}{c^2}(R_i(t_m)-R_o(t_m))^2}\cdot e^{-j2\pi f_i\left(\frac{2R_i(t_m)}{c}-\frac{2R_o(t_m)}{c}\right)}e^{j2\pi f_i\left(\frac{2R_s(t_m)}{c}-\frac{2R_o(t_m)}{c}\right)}. \quad (12)$$

According to term $\mathrm{sinc}(\bullet)$ of Eq.(12), for the scatterer i whose range is $R_i(t_m)$, the range frequency f_i and range are related by $f_i=-\frac{2\gamma}{c}(R_i(t_m)-R_o(t_m))$. Substituting f_i and $R_{\Delta so}(t_m)=R_s(t_m)-R_o(t_m)$ into Eq.(12) results in

$$S_i(f_i,t_m)=A_iT_p\mathrm{sinc}\left(T_p(f_i+2\frac{\gamma}{c}(R_i(t_m)-R_o(t_m))\right)\cdot e^{-j\frac{4\pi}{c}f_c(R_i(t_m)-R_o(t_m))}\cdot e^{j\frac{\pi}{\gamma}f_i^2}e^{j\frac{4\pi}{c}R_{\Delta so}(t_m)f_i}. \quad (13)$$

The phase compensation function of RVP and linear phase is

$$H_2(f_i,t_m)=e^{-j\frac{\pi f_i^2}{\gamma}}\cdot e^{-j\frac{4\pi}{c}R_{\Delta so}(t_m)f_i}. \quad (14)$$

After compensation the H_2, we obtain

$$S_i(f_i,t_m)=S_i(f_i,t_m)H_2(f_i,t_m)=A_iT_p\mathrm{sinc}\left(T_p(f_i+2\frac{\gamma}{c}(R_i(t_m)-R_o(t_m))\right)\cdot e^{-j\frac{4\pi}{c}f_c(R_i(t_m)-R_o(t_m))}. \quad (15)$$

The inverse Fourier transform of Eq.(15) is

$$s_i(\hat{t}_o,t_m)=A_i\mathrm{rect}\left(\frac{\hat{t}_o}{T_p}\right)\cdot e^{-j\frac{4\pi}{c}(f_c+\gamma\hat{t}_o)(R_i(t_m)-R_o(t_m))}, \quad (16)$$

where $\hat{t}_o=t-\frac{2R_o(t_m)}{c}$.

After the above processing, it can be seen from Eq.(16) that the echoed signal can be compensated to become the coherent signal dechirped with virtual center point of the target O. In order to achieve that, it needs to get accurate $R_{\Delta so}(t_m)$, while $R_{\Delta so}(t_m)$ is got from envelope alignment, and there exists error which is generally smaller than 1/4 ceil in envelope alignment, so in the following, an analysis of the influence of the envelope error is made. Suppose the estimated range difference of the dechirping reference point between the target center point is $R_{\Delta soerr}(t_m)$, which obtained by envelope alignment. the realtionship of the estimated $R_{\Delta soerr}(t_m)$ and the real $R_{\Delta so}(t_m)$ is $R_{\Delta soerr}(t_m)=R_{\Delta so}(t_m)+R_{\Delta err}(t_m)$, so the estimation error caused by envelope alignment is $R_{\Delta err}(t_m)$. Suppose the estimated range of target center O is $R_{oe}(t_m)$, according to $R_{\Delta so}(t_m)=R_s(t_m)-R_o(t_m)$ and $R_{\Delta soerr}(t_m)=R_s(t_m)-R_{oe}(t_m)$, the estimated range $R_{oe}(t_m)$ is related to the actual $R_o(t_m)$ by $R_{oe}(t_m)=R_o(t_m)-R_{\Delta err}(t_m)$. In the actual coherent processing, $R_{oe}(t_m)$ is used, so Eq.(15) is

$$S_i(f_i,t_m)=A_iT_p\mathrm{sinc}\left(T_p(f_i+2\frac{\gamma}{c}(R_i(t_m)-R_o(t_m)+R_{\Delta err}(t_m))\right)\cdot e^{-j\frac{4\pi}{c}f_c(R_i(t_m)-R_o(t_m))}\cdot e^{-j\frac{4\pi}{c}f_cR_{\Delta err}(t_m)}. \quad (17)$$

In Eq.(17) above, the initial phase term is the needed term, the second phase term is the initial phase error term which is caused by the envelope alignment error. The precision of envelope alignment is generally smaller than 1/4 resolution ceil, that is $|R_{\Delta err}(t_m)|\le\frac{1}{4}\frac{c}{2B}$, and $-\frac{4\pi}{c}f_cR_{\Delta err}(t_m)\in\frac{\pi}{2}[-\frac{f_c}{B},\frac{f_c}{B}]\bmod(2\pi)$, because of $f_c\gg B$, this phase error may be so large that it needs further compensation by autofocus. Suppose the phase compensation function is

$$H_3(f_i,t_m)=e^{j\frac{4\pi}{c}R_{\Delta err}(t_m)f_c}e^{j\phi_{err}(t_m)}, \quad (18)$$

where $\phi_{err}(t_m)$ is phase error caused by autofocus.

After the compensation of the initial phase error by multiplying $S_i(f_i,t_m)$ in Eq.(17) by $H_3(f_i,t_m)$, the inverse Fourier transform of it is

$$s_i(\hat{t}_{oe},t_m)=A_i\mathrm{rect}\left(\frac{\hat{t}_{oe}}{T_p}\right)\cdot e^{-j\frac{4\pi}{c}(f_c+\gamma\hat{t}_{oe})(R_i(t_m)-R_{oe}(t_m))}e^{j\phi_{err}(t_m)}, \quad (19)$$

where $\hat{t}_{oe}=\hat{t}-\frac{2R_{oe}(t_m)}{c}\in[-\frac{T_p}{2},\frac{T_p}{2}]$, substituting $R_{oe}(t_m)=R_o(t_m)-R_{\Delta err}(t_m)$ into Eq.(19) produces

$$s_i(\hat{t}_{oe},t_m)=A_i\mathrm{rect}\left(\frac{\hat{t}-\frac{2[R_o(t_m)-R_{\Delta err}(t_m)]}{c}}{T_p}\right)\cdot e^{-j\frac{4\pi}{c}(f_c+\gamma\hat{t}_{oe})(R_i(t_m)-R_o(t_m))-j\frac{4\pi}{c}\gamma\hat{t}_{oe}R_{\Delta err}(t_m)+j\phi_{err}(t_m)}. \quad (20)$$

After coherent processing, the sampling region of signal is $\hat{t}_{oe}$, but in theory, the sampling region what it needs is $\hat{t}_o$, thus the position error caused by sampling is $\hat{t}_{oe}-\hat{t}_o=\frac{2R_{\Delta err}(t_m)}{c}$. Because of $\left|\frac{2R_{\Delta err}(t_m)}{c}\right|\le\frac{2}{c}\frac{1}{4}\frac{c}{2B}=\frac{1}{4B}<<\frac{1}{F_s}$, in this situation, the position error caused by sampling does not exceed one sampling point. In Eq. (20), the third phase term $-\frac{4\pi}{c}\gamma\hat{t}_{oe}R_{\Delta err}(t_m)$ is the linear phase term of envelope alignment in data domain. Substituting chirp rate $\gamma=\frac{B}{T_p}$, $|R_{\Delta err}(t_m)|\le\frac{1}{4}\frac{c}{2B}$ and $\hat{t}_{oe}\in[-\frac{T_p}{2},\frac{T_p}{2}]$ into the third phase term gives $\frac{4\pi}{c}R_{\Delta err}(t_m)\gamma\hat{t}_{oe}\in\frac{\pi}{2}\frac{\hat{t}_{oe}}{T_p}\in[-\frac{\pi}{4},\frac{\pi}{4}]$, where mostly all

points are much smaller than $\frac{\pi}{4}$ and can be neglected. Finally, the comparison of Eq.(16) with Eq.(20) shows that the phase error term of actual coherent processing is

$$E(\hat{i}_{oe},t_m)=e^{-j\frac{4\pi}{c}R_{\Delta so}(t_m)\hat{i}_{oe}}e^{j\phi_{err}(t_m)}. \quad (21)$$

As it can be seen, if the errors of sampling position and phase are been ignored, Eq.(20) is equivalence to Eq.(16). In what follows, a further analysis of Eq.(16) is made in the discussion of the correction of range movement caused by rotational motion and azimuth imaging.

The equation above is the coherent processing for the targets, which meet the "stop-go" such as airplane model. For missile with high speed, this signal model is not suitable. In this condition, the influence of the target's velocity is also needed to take into account in the fast time echoed signal of range. As a result, the coherent processing of missile's signal is more complicated and it needs preprocessing. The detail discussion of that is shown in Appendix A.

3. Range Movement Correction of Scatterers

The azimuth resolution of ISAR depends on the relatively rotation of the target. The higher azimuth resolution is, the larger the rotation angle needed. Suppose the center frequency of the radar is 10GHz, bandwidth of the signal is 1GHz, the length of the wave is $\lambda=0.03m$, and thus the range resolution is $\rho_r=0.15m$. If we let the azimuth resolution ρ_a equal to the range resolution ρ_r, the rotation angle needed is about $\Delta\theta=\lambda/2\Delta\rho_a=0.1177\text{rad}=6.7418^\circ$. Suppose the cross range width of the airplane is Δx =40m, thus the maximum of MTRC is $\Delta r=\Delta\theta\cdot\Delta x/2=0.1177\times 20=2.354m$, which is much larger than range resolution. Therefore, the range movement caused by rotation must be corrected when high resolution image of the target is needed.

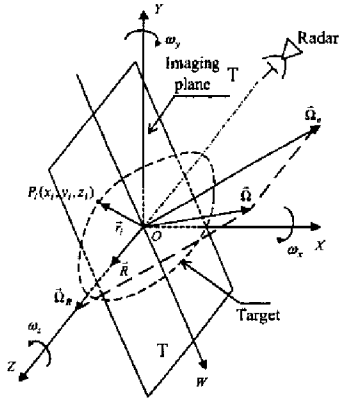

Fig.1 3-D rotating target

After the coherent processing of echoes with respect to the center point O, with the phase error neglected, the target is corresponding to be a three-dimension (3-D) rotating target shown in Fig.1.

Let $R_i(t_m)-R_o(t_m)=r_i(t_m)$, then for the i th scatterer, the range at time t_m is [24]

$$R_i(t_m)-R_o(t_m)=r_i(t_m)=r_i(0)-\int_0^{t_m}v_{ilos}(t_m)dt_m, \quad (22)$$

where v_{ilos} is the radial velocity of the i th scatterer after the target transformed to rotating target.

$$v_{ilos}=\vec{V}(t)\cdot i=-(\vec{\Omega}(t)\times\vec{r}_i(t))\cdot\vec{R}, \quad (23)$$

where $\vec{R}=[0,0,1]^T$. The range vector of the i th scatterer is

$$\vec{r}_i(t_m)=[x_i(t_m),y_i(t_m),z_i(t_m)]^T. \quad (24)$$

The rotating vector of the target is $\vec{\Omega}(t_m)$,

$$\vec{\Omega}(t_m)=[\omega_x(t_m),\omega_y(t_m),\omega_z(t_m)]^T. \quad (25)$$

The velocity vector of the i th scatterer in Eq.(23) can be simplify as

$$v_{ilos}(t_m)=\omega_y(t_m)x_i(t_m)-\omega_x(t_m)y_i(t_m). \quad (26)$$

The Taylor series expansion of $v_{ilos}(t_m)$ is

$$v_{ilos}(t_m)=v_{ilos}(0)+\dot{v}_{ilos}(0)t_m+\frac{1}{2}\ddot{v}_{ilos}(0)t_m^2. \quad (27)$$

The Taylor series expansion of $\omega_y(t_m)$, $\omega_x(t_m)$, $x_i(t_m)$ and $y_i(t_m)$ which in Eq.(26) are

$$\omega_y(t_m)=\omega_y(0)+\dot{\omega}_y(0)t_m+\frac{1}{2}\ddot{\omega}_y(0)t_m^2+\cdots, \quad (28)$$

$$\omega_x(t_m)=\omega_x(0)+\dot{\omega}_x(0)t_m+\frac{1}{2}\ddot{\omega}_x(0)t_m^2+\cdots, \quad (29)$$

$$x_i(t_m)=x_i(0)+\dot{x}_i(0)t_m+\frac{1}{2}\ddot{x}_i(0)t_m^2+\cdots, \quad (30)$$

$$y_i(t_m)=y_i(0)+\dot{y}_i(0)t_m+\frac{1}{2}\ddot{y}_i(0)t_m^2+\cdots. \quad (31)$$

Substituting Eq.(27) ~Eq.(31) into Eq.(26) results in

$$v_{ilos}(0)=\omega_y(0)x_i(0)-\omega_x(0)y_i(0), \quad (32)$$

$$\dot{v}_{ilos}(0)=[\omega_y(0)\dot{x}_i(0)+\dot{\omega}_y(0)x_i(0)-\omega_x(0)\dot{y}_i(0)-\dot{\omega}_x(0)y_i(0)], \quad (33)$$

$$\ddot{v}_{ilos}(0)=\omega_y(0)\ddot{x}_i(0)+x_i(0)\ddot{\omega}_y(0)+\dot{\omega}_y(0)\dot{x}_i(0)-\dot{\omega}_x(0)\ddot{y}_i(0)-y_i(0)\dot{\omega}_x(0)-\dot{\omega}_x(0)\dot{y}_i(0). \quad (34)$$

Substitution of Eq.(27) into Eq.(22) gives

$$\begin{aligned}r_i(t_m)&=r_i(0)-\int_0^{t_m}[v_{ilos}(0)+\dot{v}_{ilos}(0)t_m+\ddot{v}_{ilos}(0)t_m^2+\cdots]dt_m\\&=r_i(0)-[v_{ilos}(0)t_m+\frac{1}{2}\dot{v}_{ilos}(0)t_m^2+\frac{1}{6}\ddot{v}_{ilos}(0)t_m^3+\cdots]\end{aligned}. \quad (35)$$

Let $f=\gamma\hat{t}_o$ and $R_i(t_m)-R_o(t_m)=r_i(t_m)$, substituting them into Eq.(16), we get

$$S_i(f,t_m)=A_i\text{rect}\left(\frac{f}{T_p\gamma}\right)e^{-j\frac{4\pi}{c}(f_c+f)r_i(t_m)}. \quad (36)$$

Substituting $r_i(t_m)$ of Eq.(35) into Eq.(36) yieds

$$S_i(f,t_m)=A_i\text{rect}\left(\frac{f}{T_p\gamma}\right)e^{-j\frac{4\pi}{c}(f_c+f)[r_i(0)-v_{ilos}(0)t_m-\frac{1}{2}\dot{v}_{ilos}(0)t_m^2-\frac{1}{6}\ddot{v}_{ilos}(0)t_m^3+\cdots]}. \quad (37)$$

Separately writting down the high order phase term, thus $S_i(f,t_m)$ is

$$S_i(f,t_m)=A_i\mathrm{rect}\left(\frac{f}{T_p\gamma}\right)e^{-j\frac{4\pi}{c}(f_c+f)r_i(0)}e^{j\frac{4\pi}{c}(f_c+f)v_{ilos}(0)t_m}e^{j\phi_i(t_m)}, \quad (38)$$

where the high order phase term is

$$\phi_i(t_m)=\frac{4\pi}{c}(f_c+f)\left(\frac{1}{2}\dot{v}_{ilos}(0)t_m^2+\frac{1}{6}\ddot{v}_{ilos}(0)t_m^3+\cdots\right). \quad (39)$$

The term $\exp(j\frac{4\pi}{c}fv_{ilos}(0)t_m)$ in Eq.(38) represents a coupling between range and Doppler due to linear range migration of the scatterers. This range migration is the dominant bluring mechanism that must be compensated in order to obtain a high-resolution image of target [22].

We can remove the linear range migration if we rescale the time axis for each frequency by transformation. This is well-known keystone transformation that is to let $\tau_m=\frac{(f_c+f)}{f_c}t_m$.

After time scale transform, the scatterer's echoes are,

$$S_i(f,\tau_m)=A_i\mathrm{rect}\left(\frac{f}{T_p\gamma}\right)e^{-j\frac{4\pi}{c}(f_c+f)r_i(0)}e^{j\frac{4\pi}{c}f_cv_{ilos}(0)\tau_m}e^{j\phi_i(\tau_m)}, \quad (40)$$

where the high order phase term of scatterer i is

$$\phi_i(\tau_m)=\frac{4\pi}{c}(f_c+f)\left(\frac{1}{2}\dot{v}_{ilos}(0)\left(\frac{f_c}{(f_c+f)}\tau_m\right)^2+\frac{1}{6}\ddot{v}_{ilos}(0)\left(\frac{f_c}{(f_c+f)}\tau_m\right)^3+\cdots\right) \quad (41)$$

Thus, the received two dimension array signal is

$$S(f,\tau_m)=\sum_{i=1}^{Q}A_i\mathrm{rect}\left(\frac{f}{T_p\gamma}\right)e^{-j\frac{4\pi}{c}(f_c+f)r_i(0)}e^{j\frac{4\pi}{c}f_cv_{ilos}(0)\tau_m}e^{j\phi_i(\tau_m)}, \quad (42)$$

where

$$\phi_i(\tau_m)=\frac{4\pi}{c}f_c\left(\frac{1}{2}\dot{v}_{ilos}(0)\frac{f_c}{(f_c+f)}\tau_m^2+\frac{1}{6}\ddot{v}_{ilos}(0)\frac{f_c^2}{(f_c+f)^2}\tau_m^3+\cdots\right). \quad (43)$$

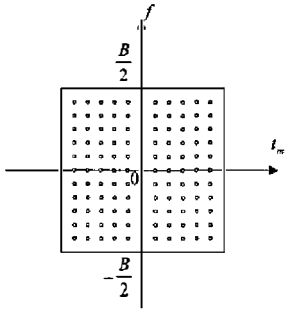

(a) Data before time scale transform (∘)

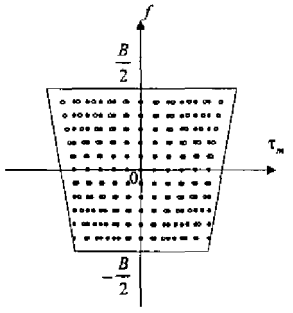

(b) Data after time scale transform (∘) and after interpolation (•)

Fig.2 Two-dimension transformation of data

Here, a time scale transform $\tau_m=\frac{f+f_c}{f_c}t_m$ is used, and the data $S(f,t_m)$ is needed to transform to $S(f,\tau_m)$, which can be achieved by interpolative sampling over again, which is shown in Fig.2. Appendix B will deal with how to realize the interpolation with FFT.

The inverse Fourier transform in range direction (f domain) results in

$$\begin{aligned}I(r,\tau_m)&=\int_{-\frac{B}{2}}^{\frac{B}{2}}S_f(f,\tau_m)e^{j\frac{4\pi f}{c}r}df\\&=\sum_{i=1}^{Q}A_i\mathrm{sinc}\left(\frac{2\gamma T_p}{c}[r-r_i(0)]\right)\cdot e^{-j\frac{4\pi}{c}f_cr_i(0)}e^{j\frac{4\pi}{c}f_cv_{ilos}(0)\tau_m}e^{j\phi_i(\tau_m)}\end{aligned} \quad (44)$$

Now that linear MTRC is compensated, time-frequency analysis for every range cell or dechirping processing is made to let the echoes to be integrated coherently.

After range compression, all frequencies are compressed upon $f=0$, however, for the time axis of $f=0$, according to $\tau_m=\frac{f+f_c}{f_c}t_m$, $\tau_m=t_m$ is got. It is that, it follows that time τ_m is equal to time t_m.

At the same time, Eq.(43) is $\phi_i(\tau_m)=\phi_i(t_m)$, and it can approximately be

$$\phi_i(\tau_m)=\phi_i(t_m)=\frac{4\pi}{c}f_c\left(\frac{1}{2}\dot{v}_{ilos}(0)t_m^2+\frac{1}{6}\ddot{v}_{ilos}(0)t_m^3+\cdots\right). \quad (45)$$

After keystone transformation and range compression, the i th scatterer's Doppler frequency at time $t_m=0$ is

$$f_{d_i}(0)=\frac{2f_c}{c}v_{ilos}(0), \quad (46)$$

in which Eq.(32) $v_{ilos}(0)=\omega_y(0)x_i(0)-\omega_x(0)y_i(0)$ has been used.

After the estimation of the Doppler frequency of the i th scatterer at time $t_m=0$, Range-Instantaneous Doppler (RID) image is obtained.

$$I(r,f_d)=\sum_{i=1}^{Q}A_i\mathrm{sinc}\left(\frac{2\gamma T_p}{c}[r-r_i(0)]\right)\cdot\mathrm{sinc}\left(T_c[f_d-\frac{2f_c}{c}v_{ilos}(0)]\right), \quad (47)$$

where T_c is the azimuth coherent integration time.

In what is to follow, an analysis of the physical meaning of the obtained image, that is the imaging plane, is made. At time 0, according to Fig.1, the difference of the i th scatterer's range and the center point O 's range is

$$\begin{aligned}r_i(0)&=\sqrt{x_i^2(0)+y_i^2(0)+(z_i(0)+R_o(0))^2}-R_o(0)\\&=z_i(0)+\frac{x_i^2(0)+y_i^2(0)}{2(z_i(0)+R_o(0))}+\cdots\approx z_i(0)\end{aligned} \quad (48)$$

In which, suppose that the target is within a sphere with radius of 30m, thus $|x_i(0)|<30m$, $|y_i(0)|<30m$. For the more, suppose $R_o(0)>1500m$, then the second term of the expansion in Eq.(48) is smaller than 0.06m which is generally smaller

than one resolution ceil (for radar whose bandwidth is 1GHz, the resolution is 0.15m), so it can be neglected. As a result, $r_i(0) = z_i(0)$, which is just the z coordinate of the i th scatterer in Fig.1.

In Eq.(46), the Doppler frequency of the i th scatterer at time $t_m = 0$ can be further written down as

$$f_{d_i}(0) = -\frac{2\sqrt{\omega_x^2(0)+\omega_y^2(0)}}{\lambda}\left[\frac{\omega_y(0)}{\sqrt{\omega_x^2(0)+\omega_y^2(0)}}x_i(0) - \frac{\omega_x(0)}{\sqrt{\omega_x^2(0)+\omega_y^2(0)}}y_i(0)\right] \quad (49)$$

Constructing the projection plane T through z axis and perpendicular to the effectual rotating component $\vec{\Omega}_e = [\omega_x(0), \omega_y(0), 0]^T$, at the same time constructing an axis W through the center O and perpendicular to z axis, which is just shown in Fig.1. Thus the coordinate of the projection point of scatterer on the projection plane T is

$$(w_i(0), z_p(0)) = \left(\frac{\omega_y(0)}{\sqrt{\omega_x^2(0)+\omega_y^2(0)}}x_i(0) - \frac{\omega_x(0)}{\sqrt{\omega_x^2(0)+\omega_y^2(0)}}y_i(0), z_i(0)\right). \quad (50)$$

By cross range scaling, multiplying $f_{d_i}(0)$ in Eq.(49) by $-\frac{\lambda}{2\sqrt{\omega_x^2(0)+\omega_y^2(0)}}$, we can obtain that its result is equal to the horizontal coordinate $w_i(0)$ of the scatterer on the projection plane T.

The analysis above indicates that the RID image obtained of the target is just the projection of the target's scatterers on the Plane T, that is the imaging plane at time $t_m = 0$ is just the projection plane T that is perpendicular to the effectual rotating component at time $t_m = 0$.

4. ISAR AZIMUTH IMAGING

In section above, after the range compression of the target's echoes, the signal has been compressed to a point in any range direction, but because of the influence of $\phi_i(\tau_m)$, in azimuth direction is it generally a nonstationary signal with modulation ratio which sometimes has more higher order term. Suppose there are P scatterers' signal in a range cell, according to Eq.(44) and Eq.(45), each azimuth echo of this range cell is

$$s(t_m) = \sum_{i=1}^{P} A_i e^{-j\frac{4\pi}{c}f_c r_i(0)} e^{j\frac{4\pi}{c}f_c v_{i_{los}}(0)t_m} e^{j\frac{4\pi}{c}f_c\left(\frac{1}{2}\dot{v}_{i_{los}}(0)t_m^2 + \frac{1}{6}\ddot{v}_{i_{los}}(0)t_m^3 + \cdots\right)} \quad (51)$$

Let $\varphi_{0i} = -j\frac{4\pi}{c}f_c r_i(0)$, $f_{0i} = \frac{2}{c}f_c v_{i_{los}}(0)$, $f_{0i} = \frac{2}{c}f_c v_{i_{los}}(0)$, $\eta_{0i} = \frac{2f_c \ddot{v}_{i_{los}}(0)}{c}$, where $f_{0i} = f_{d_i}(0)$, here it is written as f_{0i} for convenience in the following. Thus Eq.(51) is

$$s(t_m) = \sum_{i=1}^{P} A_i e^{j2\pi(f_{0i}t_m + \frac{1}{2}\mu_{0i}t_m^2 + \frac{1}{6}\eta_{0i}t_m^3 + \cdots) + j\varphi_{0i}}). \quad (52)$$

Eq.(52) also indicates that $s(t_m)$ is a nonstationary signal.

By the section above it can be concluded that it is needed to get the Doppler frequency $f_{d_i}(0)$, that is f_{0i} of any scatterer i at $t_m = 0$, as a result, it needs to estimate f_{0i} from Eq.(52). In Eq.(52), the amplitudes of the echoes of every scatterer i are equaivalent, which is impossible in practice, so we substitute $a_i(t_m)$ for A_i. Therefore, the echoes of every scatterer can be look as amplitude modulate-frequency modulate (AM-FM) signal. To a certian extent, AM-FM signal is approximate to amplitude modulate-linear frequency modulate (AM-LFM) signal, or segment AM-LFM, thus signal of any range cell in Eq.(52) is the multi-component AM-LFM signal under the noise and clutter condition. As a result, azimuth imaging is a parameter estimate problem of multi-component AM-LFM signal under the noise and clutter condition.

Therefore, for Eq.(52), it can be expressed by using a AM-LFM signal model containing P components as

$$s(t_m) = \sum_{i=1}^{P} a_i(t_m) e^{j2\pi(f_{0i}t_m + \frac{1}{2}\mu_{0i}t_m^2) + j\varphi_{0i}} + e(t_m), \quad (53)$$

where $a_i(t_m)$ is a real variable, for constant amplitude LFM signal, $a_i(t_m)$ is a constant, in which we assume that the amplitude variation is slow, and its spectrum is narrow. In fact, $s(t_m)$ is linear superimpose of multi AM-LFM component, so we only need to analysis one component, that is

$$s(t_m) = a(t_m) e^{j2\pi(f_0 t_m + \frac{1}{2}\mu_0 t_m^2) + j\varphi_0} + e(t_m). \quad (54)$$

Fourier transform of $s(t_m)$ is

$$F[s(t_m)] = e^{j\varphi_0} F[a(t_m)] \otimes \delta(f - f_0) \otimes F[e^{j\pi\mu_0 t_m^2}] + F[e(t_m)]. \quad (55)$$

Because the variation of $a(t_m)$ is slow, $F[a(t_m)]$ is a narrow spectrum centered in zeros frequency. $\delta(f - f_0)$ is modulation, which will shift the spectrum, $F[e^{j\pi\mu_0 t_m^2}]$ is the spectrum of chirp factor, the greater μ_0 is, the wider spectrum is.

It is usually to use dechirping method to estimate chirp rate μ_0, that is multiply $s(t_m)$ by negative chirp rate factor $e^{-j\frac{1}{2}\kappa t_m^2}$, which results in

$$f_\gamma(t_m) = s(t_m) e^{-j\frac{1}{2}\kappa t_m^2}. \quad (56)$$

If $\kappa = \mu_0$, then $f_\gamma(t_m) = a(t_m) e^{j2\pi f_0 t_m + j\varphi_0}$, the Fourier transform of $f_\gamma(t_m)$ is $F[f_r(t_m)] = e^{j\varphi_0} F[a(t_m)] \otimes \delta(f - f_0)$, which is a narrow spectrum around initial frequency f_0. From the position of peak, f_0 is estimated. The search method of f_0 is: change κ, and do FFT for each $f_\gamma(t_m)$, and draw two dimensional distribution along initial frequency f_0 and chirp rate κ, and estimate two parameter f_0 and μ_0 of LFM component from the peak.

After estimated initial frequency f_0 and chirp rate μ_0, dechirping the original component and shift it to zero frequency, then

$$y(t_m)=s(t_m)e^{-j2\pi(f_0t_m+\frac{1}{2}\mu_0t_m^2)}=a(t_m)e^{j\varphi_0}+e(t_m)e^{-j2\pi(f_0t_m+\frac{1}{2}\mu_0t_m^2)} \quad (57)$$

By Fourier transform, the phase of zero frequency is the estimation of φ_0. By filter the narrow spectrum around zero frequency, and do inverse Fourier transform, the estimation of $a(t_m)$ is obtained, in order to reduce sidelobe, taylor or hamming window is needed when do Fourier transform and after inverse Fourier transform it is needed to divide the result by window coefficient.

For multi-component AM-LFM signal, many peaks are emerged in two dimensional distribution map (the initial frequency f and chirp rate κ), according to the position of peaks, the estimation of f_{0_i} and μ_{0i} are obtained. At these peaks' position, filter the narrow spectrum along the initial frequency f direction, shift it to center, and do inverse Fourier transform, the estimation of each component $a_i(t_m)$ is obtained.

Because the search of the initial frequency f and chirp rate κ in two dimension is time consuming, especially the higher precision of κ is, the greater search computation load is, so we adopt "clean" method to estimate AM-LFM component from great to small.

Suppose one range cell signal is composed by P AM-LFM components and white noise, the slow time $t_m=mT$, where T is pulse repetition period, so the signal $s(t_m)$ can be written as,

$$s(mT)=\sum_{i=1}^{P}a_i(mT)e^{j2\pi f_{0_i}mT+j\pi\mu_{0_i}(mT)^2+j\varphi_{0i}}+e(mT),\ m=1,\cdots,M. \quad (58)$$

The k th AM-LFM component's initial frequency f_{0k} and chirp rate μ_{0_k} are determined by the peak of two dimensional distribution $C(f,\kappa)$ of $s_{k-1}(mT)$,

$$C(f,\kappa)=\sum_{m=1}^{M}\{[s_{k-1}(mT)\cdot e^{-j2\pi f_{0_i}mT-j\pi\kappa(mT)^2}]\}/M, \quad (59)$$

$$\{\hat{f}_{0k},\hat{\mu}_{0k}\}=\arg\max\{|C(f,\kappa)|\}, \quad (60)$$

where $s_{k-1}(mT)$ is remainder signal obtained by subtracting the estimated $k-1$ AM-LFM components from original signal, and where arg expresses to get the independent variable of the function. The estimate of f_{0_k} and μ_{0_k} can be obtained quickly by utilizing FFT.

$$\{\hat{f}_{0k},\hat{\mu}_{0k}\}=\max_{\kappa}\{\max_{f}\{\mathrm{FFT}[s_{k-1}(mT)\cdot e^{-j\pi\kappa(mT)^2}/M]\}\}. \quad (61)$$

The initial phase is the phase of peak,

$$\hat{\varphi}_{0k}=\angle C(\hat{f}_{0k},\hat{\mu}_{0k}), \quad (62)$$

where $\angle$ expresses to get angle.

Suppose $\mathrm{Win}_k(f)=\begin{cases}1 & f_{Lk}<f<f_{Rk}\\ 0 & \text{else}\end{cases}$ is filtering window of k th component in frequency domain, and $f_{Rk}>0$, $f_{Lk}<0$, whose value is determined by spectral width of peak which is shifted to zeros. The discrete form of $\mathrm{Win}_k(f)$ can be written as $\mathrm{Win}_k(\frac{m}{MT})$. The time variation amplitude is IFFT module of filtered spectrum peak, which is shifted to zero frequency, that is,

$$\hat{a}_k(mT)=\left|\mathrm{IFFT}\{\mathrm{Win}_k(\tfrac{m}{MT})\cdot\mathrm{FFT}[s_{k-1}(mT)\cdot e^{-j\hat{\Phi}_k(mT)-j\hat{\varphi}_{0k}}]\}\right|. \quad (63)$$

where $\hat{\Phi}_k(mT)=2\pi\hat{f}_{0k}mT+j\pi\hat{\mu}_{0k}(mT)^2$.

After subtracting k th AM-LFM component in frequency domain from $s_{k-1}(mT)$, $s_k(mT)$ is obtained,

$$s_k(mT)=\mathrm{IFFT}\{[1-\mathrm{Win}_k(\tfrac{m}{MT})]\cdot\mathrm{FFT}[s_{k-1}(mT)e^{-j\hat{\Phi}_k(mT)}]\}\cdot e^{j\hat{\Phi}_k(mT)} \quad (64)$$

Now, we give the step of AM-LFM signal's parameter estimation method as follow:

Step(1): $k=1$, that is $s_0(mT)=s(mT)$, according to Eqs. (61), (62) and (63) the first AM-LFM component's initial frequency, chirp rate, initial phase and time variant amplitude are estimated, then according to Eq.(64) the reminder signal $s_1(mT)$ is obtained by subtracting this AM-LFM component from original signal.

Step(2): $k=2$, according to Eqs. (61), (62) and (63) the second AM-LFM component's initial frequency, chirp rate, initial phase and time variant amplitude are estimated, then by subtracting the second AM-LFM component from $s_1(mT)$ according to Eq.(64), the reminder signal $s_2(mT)$ is obtained.

Remaining steps: when $k=K$, according to Eqs. (61), (62) and (63), the K th AM-LFM component's parameters are estimated, then subtracting the K th AM-LFM component from $s_{k-1}(mT)$ according to Eq.(64), the remainder signal $s_K(mT)$ is obtained. If the reminder signal's energy is small enough, or K reaches the required component number P, the iterative is end.

In the estimation processing, expect κ needed searching, else parameters only need simple FFT, getting maximum and multiplying, so it is easy to realize and the computer efficiency is high. Moreover, the parameter μ_{0k} can be searched step by step to reduce computation load, each step have eleven points, usually it only needs to search three or four steps.

5. Block Diagram of ISAR Imaging Algorithm

The key to the high-resolution imaging is that the range

movement caused by rotational motion must be compensated. When the target is rotating, the scatterers' range movement rates are different, and keystone transformation can correct range movement with different rate at the same time, but it is demanded the signal before keystone transformation be coherent. In this paper, ISAR echoes is first to be make coherent with virtual center O of the target, so that the target can be treated as a three-dimensional rotating target that is rotating with respect to the virtual center O, which is equivalent to the dechiping referent point. Secondly, the range movement correction is done. For the range alignment with virtual center O, many envelope alignment algorithms, such as amplitude correlation method and minimum entropy method, can be used to estimate $R_{\Delta so}(t_m)$ which is used in phase compensation function H_1 and H_2. For autofocus, many autofocus algorithms such as multiple PPP algorithm and PGA can be used to estimate phase compensation function H_3. In conventional translational motion compensation (TMC), phase compensation function H_2 does not do, that is, rawdata envelopes usually need not to compensation.

After coherent processing with the virtual center O, for a steadily flying target, the target's rotation is uniform and planar, the received data is same to the data received by a spotlight SAR in polar format, so the polar formation is usually used. But for a non-cooperative target, the rotation is usually nonuniform and three-dimensional (pitch, roll and yaw), as a result, the polar format algorithm is not suitable. For this situation, keystone transformation is used to correct MTRC, certainly, it only correct linear range migration and can not completely correct MTRC. After the range compression, the time-frequency analysis is made to estimate scatterers' instantaneous Doppler frequencies for each range cell. Finally, the target's RID image is obtained.

Fig.3 shows the block diagram of ISAR echoes coherent processing and imaging algorithm for maneuvering target high resolution ISAR processing.

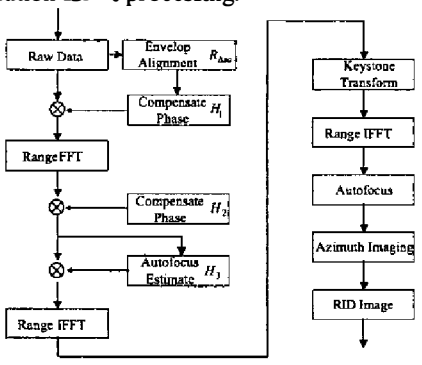

Fig.3 Block diagram of ISAR echoes coherent processing and imaging algorithm for maneuvering target high resolution ISAR imaging

6. ISAR IMAGING OF SIMULATION DATA

In what follows, there is an example of ISAR imaging of simulation data. It is a Yak-42 aircraft model with 330 scatterers shown in Fig.4, and its length, width and height is separately 70m, 60m and 9m. The radar center frequency is 10GHz, bandwidth is 1000MHz, pulse repeat frequency (PRF) is 50Hz, and the fast time (range direction) sample rate is 40MHz. The model is flying in a curve, and the target range is 400 kilometer. The range measuring precision is ±10m, that is say, the position error of dechirp reference signal and target center is within ±10m.

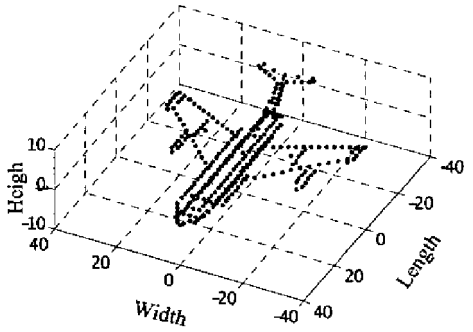

Fig.4 Three-dimensional view diagram of simulation Yak-42 aircraft

Fig.5(a) shows the simulation data in the range fast time and azimuth slow time domain after receiver dechirping processing. In Fig.5(b) the envelope of range image after IFFT is shown, and because the referent signal is not accurately tracking the target's center, the range image is saltant and not align. Fig.5(c) shows the RD image obtain by conventional motion compensation that is range image envelope alignment and autofocus. As it is shown, the scatterers are defocus seriously and form a slant line. It also shows that the MTRC of scatterers exits and the azimuth Doppler varies with time. After the range image envelope alignment and autofocus, returning to the range fast time and azimuth slow time domain, but without phase compensation H_2, that is there is not the translational motion correction of rawdata's envelope, keystone transformation is done to correct the range movement, the range image obtained in Fig.5(d). In this condition, because the raw range is not completely coherent, keystone interpolation is not accurate, and the envelope is disorder, the ratio of signal to noise is low. Fig.5(e) shows the general RD image of the Fig.(d) data. Fig.5(f) is the RID image of the Fig.(d) data using AM-FM signal parameter estimation method proposed in the paper to estimate instantaneous Doppler parameter. As it is shown, the image is bad. Fig.5(g) is RD image after completely coherent processing but without MTRC, this image is more better than Fig.5(c), but defocus and range movement are still exist. Fig.5(h) is the

range image after completely coherent processing and keystone transformation. The range movement of the scatterers is eliminated. Fig.5(i) is the RD image of Fig.5(h) data, comparison of Fig.5(c) with Fig.5(i) shows that in Fig.5(i) the scatterers are defocus only in cross range direction, it can show than the range movement is eliminated but the Doppler frequency is still time-variable. Fig.5(j) is the RID image of Fig.5(h) after azimuth imaging using AM-LFM parameter estimation method, that is, Fig.5(i) is the finally RID image result of simulation data with the block diagram processing of Fig.3. As we can see, the imaging result is very good.

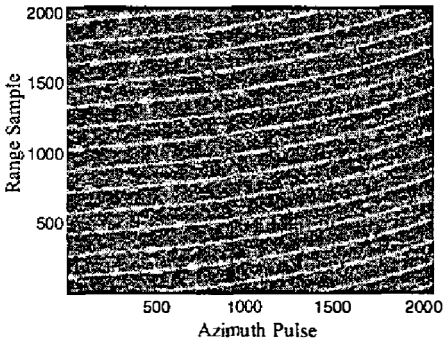

Fig.5(a) Simulation data

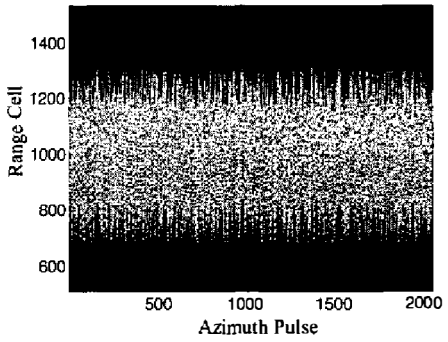

Fig.5(b) Range image of simulation data

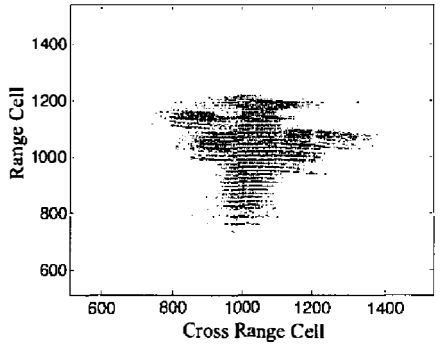

Fig.5(c) RD Image after conventional TMC

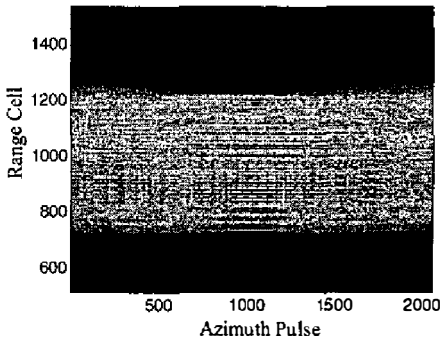

Fig.5(d) Range image after conventional TMC and keystone transformation

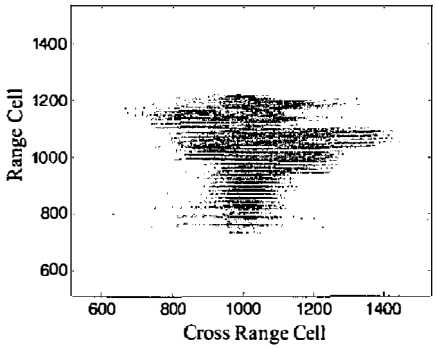

Fig.5(e) RD image of Fig.5(d)

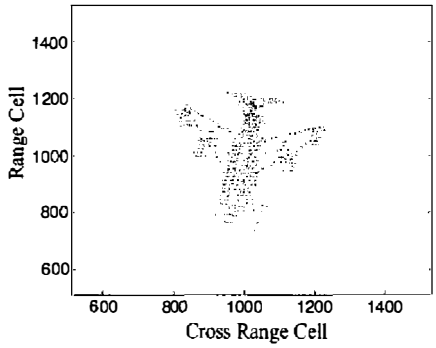

Fig.5(f) RID image of Fig.5(d)

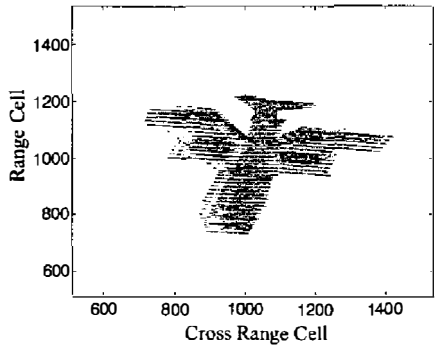

Fig.5(g) RD image after coherent processing but without MTRC

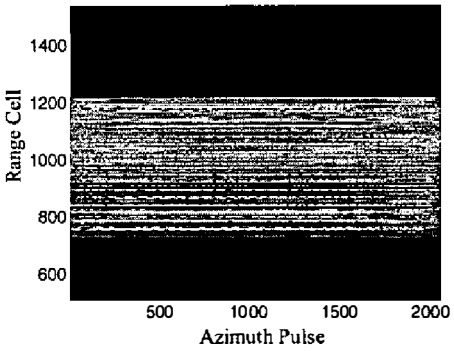

Fig.5(h) Range image after coherent processing and keystone transformation

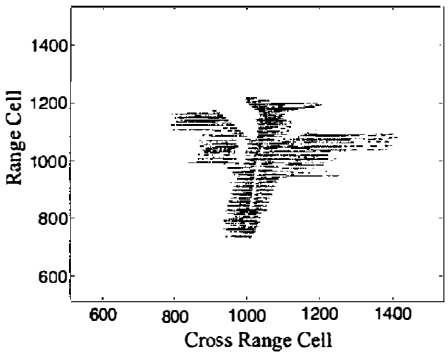

Fig.5(i) RD image of Fig.5(h)

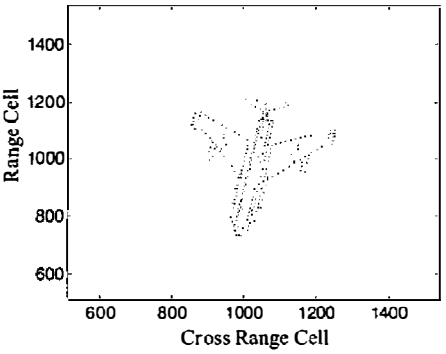

Fig.5(j) RID image of Fig.5(h)

Fig.5 Coherent processing and imaging of ISAR simulation data

7. Conclusion

In the ISAR imaging with high resolution, after the translational motion compensation of the target, the MTRC caused by rotational motion is also needed to be compensation. Because the target is non-cooperative, and the rotating angle of the target is nonuniform and three-dimensional, it is not suitable for the polar formation algorithm. In this paper, keystone transformation proposed in SAR imaging for moving target is used to correct the linear range migration caused by rotation.

Because the dechirp referent point of the ISAR rawdata varies with the movement of the target, moreover it is difficult to precisely tracking the target center, the rawdata is not coherent.

In this paper, the rawdata is separately phase compensated in time domain and frequency domain to make it coherent, it is that, on the basis of the general ISAR imaging in which only the envelope alignment of rang image and the autofocus are done, we multiply the data by the linear phase in rang image domain to make the envelope of raw returned data also align, so the raw returned data is completely coherent. In the next, the keystone transformation is done to correct linear MTRC. After the correction of MTRC and compression of range, a parameter estimation method of multicomponent amplitude modulation and linear frequency modulation(AM-LFM) signal is finally proposed to estimate the scatterer's instantaneous amplitudes and frequencies, and the instantaneous ISAR image is obtained.

Appendix A. The Preprocessing for The Echoes of Missile With High Speed

ISAR Echoes Coherent Processing for Missile

Echoes of the target belongs to airplane class meet the "stop-go" model, while for the missile with high speed, the model does not work, in this case, the velocity of the target is also needed to take into acount in range fast time.

Suppose the transmitted signal of the radar is the same as the analysis above, which is

$$s(\hat{t},t_m)=\mathrm{rect}\left(\frac{\hat{t}}{T_p}\right)e^{j2\pi(f_c\hat{t}+\frac{1}{2}\gamma\hat{t}^2)}, \qquad \text{(A-1)}$$

where $\mathrm{rect}(u)=\begin{cases}1 & |u|\le\frac{1}{2}\\ 0 & |u|>\frac{1}{2}\end{cases}$, f_c is center frequency, T_p is pulse width, γ is the frequency modulation rate, $\hat{t}=t-mT$ is fast time, m is an integral number, T is repetition period, $t_m=mT$ is slow time.

Suppose the target have Q scatterers, the range of i th scatterer from radar at time $(t_m,\hat{t})$ is $R_i(\hat{t},t_m)=R_i(t_m)+V_{Ti}\hat{t}$, the received data

$$s_R(\hat{t},t_m)=\sum_i^Q A_i\mathrm{rect}\left(\frac{\hat{t}-2R_i(\hat{t},t_m)/c}{T_p}\right)e^{j2\pi\left(f_c\left(t-\frac{2R_i(\hat{t},t_m)}{c}\right)+\frac{1}{2}\gamma\left(\hat{t}-\frac{2R_i(\hat{t},t_m)}{c}\right)^2\right)} \qquad \text{(A-2)}$$

where c is the velocity of light. Because the echoes of every scatterers are independent, so the echo $s_{iR}(\hat{t},t_m)$ of i th scatterer is first be studied, it is

$$s_{iR}(\hat{t},t_m)=A_i\mathrm{rect}\left(\frac{\hat{t}-2R_i(\hat{t},t_m)/c}{T_p}\right)e^{j2\pi\left(f_c\left(t-\frac{2R_i(\hat{t},t_m)}{c}\right)+\frac{1}{2}\gamma\left(\hat{t}-\frac{2R_i(\hat{t},t_m)}{c}\right)^2\right)} \qquad \text{(A-3)}$$

where the range of this scatterer from radar is $R_i(t,t_m)$.

The reference signal is

$$s_{ref}(\hat{t},t_m)=e^{j2\pi\left(f_c\left(t-\frac{2R_s(t_m))}{c}\right)+\frac{1}{2}\gamma\left(\hat{t}-\frac{2R_s(t_m)}{c}\right)^2\right)}. \quad \text{(A-4)}$$

After dechirp, the output is

$$\begin{aligned}s_{if}(\hat{t},t_m)&=s_{iR}(\hat{t},t_m)\cdot s_{ref}^{*}(\hat{t},t_m)\\&=A_i\mathrm{rect}\left(\frac{\hat{t}-2R_i(\hat{t},t_m)/c}{T_p}\right)\\&\quad e^{-j\frac{4\pi}{c}\left(f_c+\gamma(\hat{t}-\frac{2R_s(t_m)}{c})\right)(R_i(\hat{t},t_m)-R_s(t_m))}\,e^{j\frac{4\pi\gamma}{c^2}(R_i(\hat{t},t_m)-R_s(t_m))^2}\\&=A_i\mathrm{rect}(\cdot)e^{j(\Phi_1(\hat{t},t_m)+\Phi_1(\hat{t},t_m)+\Phi_2(\hat{t},t_m))}\end{aligned} \quad \text{(A-5)}$$

where,

$$\begin{aligned}\Phi_1(\hat{t},t_m)=&-\frac{4\pi}{c}\{f_c[R_i(t_m)-R_s(t_m)]\\&+[f_c-\gamma\frac{2[R_i(t_m)-R_s(t_m)]}{c}-\frac{V_T}{c}\gamma\frac{2R_s(t_m)}{c})V_T\frac{2R_s(t_m)}{c}\}\end{aligned} \quad \text{(A-6)}$$

$$\begin{aligned}\Phi_2(\hat{t},t_m)=&-\frac{4\pi}{c}\{[R_i(t_m)-R_s(t_m)]+[(\frac{f_c}{\gamma}-\frac{2[R_i(t_m)-R_s(t_m)]}{c}\\&+(1-\frac{2V_T}{c})\frac{2R_s(t_m)}{c})V_T]\}\cdot\gamma(\hat{t}-\frac{2R_s(t_m)}{c})\end{aligned} \quad \text{(A-7)}$$

$$\Phi_3(\hat{t},t_m)=\frac{4\pi}{c^2}\gamma[R_i(t_m)-R_s(t_m)]^2+\frac{4\pi}{c}\gamma(\frac{V_T}{c}-1)V_T(\hat{t}-\frac{2R_s(t_m)}{c})^2 \quad \text{(A-8)}$$

where $\Phi_1(\hat{t},t_m)$ is initial phase, $\Phi_2(\hat{t},t_m)$ is the term that expresses the position information, $\Phi_3(\hat{t},t_m)$ is residual video phase (RVP) and the second order phase term for fast time. $(\frac{f_c}{\gamma}-\frac{2R_i(t_m)}{c}+2(1-\frac{V_T}{c})\frac{2R_s(t_m)}{c})V_T$ in $\Phi_2(\hat{t},t_m)$ produces the range image shift, $\frac{4\pi}{c^2}\gamma[R_i(t_m)-R_s(t_m)]^2$ in $\Phi_3(\hat{t},t_m)$ is the term called RVP which does not effect the width of range image, the second term $\frac{4\pi}{c}\gamma(\frac{V_T}{c}-1)V_T(\hat{t}-\frac{2R_s(t_m)}{c})^2$ in $\Phi_3(\hat{t},t_m)$ widens the spectrum of range image.

Let $\Phi_1(\hat{t},t_m)=\Phi_{1a}(\hat{t},t_m)+\Phi_{1c}(\hat{t},t_m)+\Phi_{1c}(\hat{t},t_m)$, where

$$\Phi_{1a}(\hat{t},t_m)=-\frac{4\pi}{c}f_c[R_i(t_m)-R_s(t_m)], \quad \text{(A-9)}$$

$$\Phi_{1b}(\hat{t},t_m)=-\frac{4\pi}{c}[f_c-\frac{V_T}{c}\gamma\frac{2R_s(t_m)}{c}]V_T\frac{2R_s(t_m)}{c}, \quad \text{(A-10)}$$

$$\Phi_{1c}(\hat{t},t_m)=\frac{4\pi}{c}\gamma\frac{2[R_i(t_m)-R_s(t_m)]}{c}V_T\frac{2R_s(t_m)}{c}. \quad \text{(A-11)}$$

Let $\Phi_2(\hat{t},t_m)=\Phi_{2a}(\hat{t},t_m)+\Phi_{2b}(\hat{t},t_m)+\Phi_{2c}(\hat{t},t_m)$, where

$$\Phi_{2a}(\hat{t},t_m)=-\frac{4\pi}{c}[R_i(t_m)-R_s(t_m)]\cdot\gamma(\hat{t}-\frac{2R_s(t_m)}{c}), \quad \text{(A-12)}$$

$$\Phi_{2b}(\hat{t},t_m)=-\frac{4\pi}{c}[(\frac{f_c}{\gamma}+(1-\frac{2V_T}{c})\frac{2R_s(t_m)}{c})V_T]\cdot\gamma(\hat{t}-\frac{2R_s(t_m)}{c}), \quad \text{(A-13)}$$

$$\Phi_{2c}(\hat{t},t_m)=\frac{4\pi}{c}\frac{2[(R_i(t_m)-R_s(t_m)]}{c}\cdot V_T\cdot\gamma(\hat{t}-\frac{2R_s(t_m)}{c}), \quad \text{(A-14)}$$

where $\Phi_{2c}(\hat{t},t_m)=\Phi_{2c1}(\hat{t},t_m)+\Phi_{2c2}(\hat{t},t_m)$, which can be divided into two components,

$$\Phi_{2c1}(\hat{t},t_m)=\frac{4\pi}{c}\frac{2[(R_i(t_m)-R_o(t_m)]}{c}\cdot V_T\cdot\gamma(\hat{t}-\frac{2R_s(t_m)}{c}), \quad \text{(A-15)}$$

$$\Phi_{2c2}(\hat{t},t_m)=-\frac{4\pi}{c}\frac{2[(R_s(t_m)-R_o(t_m)]}{c}\cdot V_T\cdot\gamma(\hat{t}-\frac{2R_s(t_m)}{c}), \quad \text{(A-16)}$$

where $\Phi_{2c1}(\hat{t},t_m)$ is the coupling phase of fast time and slow time, and $\Phi_{2a}(\hat{t},t_m)$ is also coupling term, but its coupling coefficient is only $2V_T/c$ times $\Phi_{2a}(\hat{t},t_m)$. Suppose V_T=4500m/s, then $2V_T/c$ =0.0003 that is very small, so the coupling term of $\Phi_{2c1}(\hat{t},t_m)$ can be neglected. The linear phase of $\Phi_{2c2}(\hat{t},t_m)$ brings about the range image shift. Suppose the error of $R_{\Delta so}(t_m)=R_s(t_m)-R_o(t_m)$ is 60m, as the same, V_T is 5000m/s, the translational motion error of range image is $R_{\Delta so}(t_m)V_T/c$ that is equal to 0.001m, which can be neglected.

Let $\Phi_3(\hat{t},t_m)=\Phi_{3a}(\hat{t},t_m)+\Phi_{3b}(\hat{t},t_m)$, where

$$\Phi_{3a}(\hat{t},t_m)=\frac{4\pi}{c^2}\gamma[R_i(t_m)-R_s(t_m)]^2, \quad \text{(A-17)}$$

$$\Phi_{3b}(\hat{t},t_m)=\frac{4\pi}{c}\gamma(\frac{V_T}{c}-1)V_T(\hat{t}-\frac{2R_s(t_m)}{c})^2, \quad \text{(A-18)}$$

The comparison of those with Eq.(6) shows that $\Psi_a(\hat{t},t_m)=\Phi_{1a}(\hat{t},t_m)+\Phi_{2a}(\hat{t},t_m)+\Phi_{3a}(\hat{t},t_m)$ is the whole phase term of general target with low speed.

Firstly the initial phase cause by high speed target, the linear phase that brings about range image shift and the second order phase term that widen range image's spectrum are compensated, and the compensating function is constructed as

$$H_{m1}(\hat{t},t_m)=\exp\{-j[\Phi_{1b}(\hat{t},t_m)+\Phi_{2b}(\hat{t},t_m)+\Phi_{3b}(\hat{t},t_m)]\}. \quad \text{(A-19)}$$

Suppose the referent dechirping range of rawdata is $R_s(t_m)$, in order to compensate it to dechirped signal with referent range $R_o(t_m)$, construct the phase compensating function H_1 as

$$H_1(\hat{t},t_m)=\exp\left\{-j\frac{4\pi}{c}(f_c+\gamma\hat{t}_s)R_{\Delta so}(t_m)-j\frac{4\pi\gamma}{c^2}(R_{\Delta so}(t_m))^2\right\} \quad \text{(A-20)}$$

After the compensation of raw signal with $H_{m1}(\hat{t},t_m)$ and $H_1(\hat{t},t_m)$, FFT on $\hat{t}_s=\hat{t}-\frac{2R_s(t_m)}{c}$ can obtain

$$\begin{aligned}S_i(f_i,t_m)=&A_iT_p\mathrm{sinc}\left(T_p(f_i+2\frac{\gamma}{c}(R_i(t_m)-R_o(t_m))\right)\cdot\\&e^{-j\frac{4\pi}{c}f_c(R_i(t_m)-R_o(t_m))}\cdot e^{j\frac{\pi}{\gamma}f_i^2}e^{j\frac{4\pi}{c}R_{\Delta so}(t_m)f_i}e^{j\Phi_{1c}(f_i,t_m)}\end{aligned}, \quad \text{(A-21)}$$

where

$$\begin{aligned}\Phi_{1c}(\hat{t},t_m)=&\frac{4\pi}{c}\gamma\frac{2[R_i(t_m)-R_o(t_m)]}{c}V_T\frac{2R_s(t_m)}{c}\\&+\frac{4\pi}{c}\gamma\frac{2[R_o(t_m)-R_s(t_m)]}{c}V_T\frac{2R_s(t_m)}{c}\\=&\frac{4\pi}{c}\gamma\frac{2[R_i(t_m)-R_o(t_m)]}{c}V_T\frac{2R_s(t_m)}{c}\\&-\frac{4\pi}{c}\gamma\frac{2R_{\Delta so}(t_m)}{c}V_T\frac{2R_s(t_m)}{c}\end{aligned}, \quad \text{(A-22)}$$

using $f_i=-\frac{2\gamma}{c}(R_i(t_m)-R_o(t_m))$, $\Phi_{1c}(\hat{t},t_m)$ can be transformed

into $\Phi_{1c}(f_i,t_m)$ in frequency domain

$$\Phi_{1c}(f_i,t_m)=-\frac{4\pi}{c}f_iV_T\frac{2R_s(t_m)}{c}-\frac{4\pi}{c}\gamma\frac{2R_{\Delta so}(t_m)}{c}V_T\frac{2R_s(t_m)}{c}. \quad \text{(A-23)}$$

The compensating function to compensate the linear phase in frequency domain is

$$H_{m2}(f_i,t_m)=\exp\{-j\Phi_{1c}(f_i,t_m)\}. \quad \text{(A-24)}$$

The following processing is the same as the steps behind Eq.(14) of the general target. In finally, Eq.(16) is obtained by compensating. If $\Phi_{2c1}(\hat{t},t_m)$ is not neglected, the signal after coherent processing is

$$s_i(\hat{t}_o,t_m)=A_i rect\left(\frac{\hat{t}_o}{T_p}\right)\cdot e^{-j\frac{4\pi}{c}(f_c+(1-\frac{2V(t)}{c})\gamma\hat{t}_o)(R_i(t_m)-R_o(t_m))}. \quad \text{(A-25)}$$

While if $\Phi_{2c1}(\hat{t},t_m)$ is neglected, the signal after coherent processing is

$$s_i(\hat{t}_o,t_m)=A_i rect\left(\frac{\hat{t}_o}{T_p}\right)\cdot e^{-j\frac{4\pi}{c}(f_c+\gamma\hat{t}_o)(R_i(t_m)-R_o(t_m))}. \quad \text{(A-26)}$$

The Velocity Estimate Method for Missile

The analysis before shows that it is needed to know the target's velocity in the beforehand coherent processing of the missile with high speed. The target's velocity can be obtained by two methods: 1) estimate from dechirp reference ranges; 2) estimate from the frequency modulation rate of every range image whose spectrum has widened, that is, estimate from Φ_{3b} in Eq.(A-18) (where Φ_{3b} can generally be approximate to $\Phi_{3b}(\hat{t},t_m)=-\frac{4\pi}{c}\gamma V_T(\hat{t}-\frac{2R_s(t_m)}{c})^2$), and the frequency modulation rate of every range image can be estimated by MD method that is usually used in SAR imaging [8]. Suppose the unitary frequency modulation rate estimated from the m th range image is $k(m)$, then the actual frequency modulation rate is $k_r(m)=k(m)\cdot F_s^2$, where F_s is range sampling rate. As a result, the estimated velocity of the target at slow time $t_m=mT$ is

$$V_e(t_m)=-\frac{k_r(m)\cdot c}{4\gamma}. \quad \text{(A-27)}$$

After the velocity estimation from all range images, it is needed to use second order or third order curve-fitting to promote the precision of velocity estimation

APPENDIX B. FAST REALIZATION OF KEYSTONE TRANSFORMATION

Realize keystone transformation by DFT-IFFT

According to Eq.(38), the radar received i th scatterer's echoes after dechirping are

$$S_i(f,t_m)=A_i\text{rect}\left(\frac{f}{T_p\gamma}\right)e^{-j\frac{4\pi}{c}(f_c+f)r_i(0)}e^{j\frac{4\pi}{c}(f_c+f)v_{iLos}(0)t_m}e^{j\phi_i(t_m)}. \quad \text{(B-1)}$$

Because i th scatterer's frequency is $f_{d_i}=-\frac{2v_{iLos}(0)}{\lambda}=-\frac{2f_cv_{iLos}(0)}{c}$, and the pulse width is wide, Eq.(B-1) can be simplified as,

$$S_f(f,t_m)=\sum_{i=1}^{Q}A_ie^{-j\frac{4\pi}{c}(f_c+f)r_i(0)}e^{j2\pi(1+\frac{f}{f_c})f_{d_i}t_m}. \quad \text{(B-2)}$$

Because in fact the received data is discrete, so Eq.(B-2) can be written as,

$$S(n,m)=\sum_{i=1}^{Q}\tilde{A}_ie^{-j2\pi\rho_in}e^{j2\pi(1+\eta n)f_im}. \quad \text{(B-3)}$$

where $\rho_i=\frac{r_i(0)}{c}\frac{B}{N}$, $f_i=f_{d_i}T$, $\eta=\frac{B}{f_cN}$, $\tilde{A}_i=A_ie^{-j\frac{4\pi}{c}f_cr_i(0)}$.

DFT and IFFT transform is done on m coordinate, so Eq.(B-3) can be rewritten as,

$$S(n,m')=\sum_{l=-\frac{M}{2}}^{l=\frac{M-1}{2}}\left(\sum_{m=-\frac{M}{2}}^{m=\frac{M-1}{2}}S(n,m)e^{-j\frac{2\pi(1+\eta n)}{M}lm}\right)e^{j\frac{2\pi}{M}lm'}, \quad \text{(B-4)}$$

where $l=[-\frac{M}{2}],[-\frac{M}{2}]+1,\cdots,[\frac{M-1}{2}]$, $m'=[-\frac{M}{2}],[-\frac{M}{2}]+1,\cdots,[\frac{M-1}{2}]$, and [] denotes rounding.

The transform of $S(n,m)$ into $S(n,m')$ just is keystone transformation.

Realize Keystone Transformation by SFT-IFFT

Suppose $s(t)$ and $s(f)$ is the Fourier pair, the

$$s(t)\overset{FFT}{\bullet\!\!\rightarrow}s(f). \quad \text{(B-5)}$$

The time scaled Fourier transform is,

$$s(t)\overset{SFT}{\bullet\!\!\rightarrow}s(b,f)=\int s(t)e^{-j2\pi bft}dt. \quad \text{(B-6)}$$

This transform can be realized with chirps as shown in Fig.B-1. For Eq.(B-6), $b=(1+\eta n)$.

The realization of Eq.(B-4) using SFT-IFFT transform as shown in Fig.B-2, where time domain convolution is realized by frequency domain multiplication.

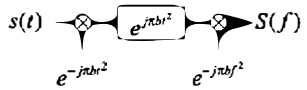

Fig.B-1 Time scaled Fourier transform realized with chirps

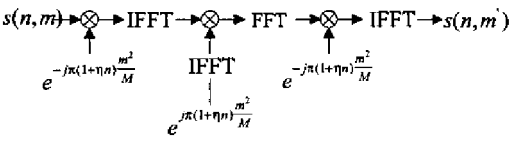

Fig.B-2 The diagram of keystone interpolation realized by SFT-IFFT

ACKNOWLEDGMENTS

The authors would like to thank the reviewers for their helpful comments and suggestions.

This work is partially supported by the National Science Foundation of China (No.69831040) and the National Defense Pre-research Foundation of China (No:413070502, No:40106020101).

REFERENCES

[1] [Ausherman, D.A., Kozma, A., Walker, J.L., Jones, H. M., and Poggio, E.C. "Developments in radar imaging," *IEEE Transaction on Aerospace and Electronic System*, Vol.20, No.4, pp.363-400, July 1984

[2] C. C. Chen ,H. C. Andrews, "Target-Motion-Induced Radar Imaging," *IEEE Transactions on Aerospace and Electronic System*, Vol.16, No 1, pp.2-14, 1980

[3] Delisle, G.Y., and Wu.H. (1994) "Moving target imaging and trajectory computation using ISAR," *IEEE Transaction on Aerospace and Electronic Systems*, Vol.30, No.3, pp. 887-889, July 1994

[4] Junfeng Wang; Kasilingam, D. "Global range alignment for ISAR", Aerospace and Electronic Systems, IEEE Transactions on, Volume: 39 Issue: 1 , Jan 2003, Page(s): 351 –357.

[5] Steinberg, B.D, "Microwave imaging of aircraft," *Proceedings of IEEE*, Vol.76, No.12, pp.1578-1592, 1988.

[6] Berizzi, F.; Pinelli, G., "Maximum-likelihood ISAR image autofocusing technique based on instantaneous frequency estimation," *Radar, Sonar and Navigation, IEE Proceedings* - , Vol.144, No.5, pp. 284 –292, Oct. 1997.

[7] Itoh, T., Sueda, H., and Watanabe, Y, "Motion compensation for ISAR via centroid tracking," *IEEE Trans. on AES*, Vol.32, No.3, pp. 1191-1197, July 1996.

[8] Walter G. Carrara, Ron S. Goodman, Ronald M. Majewski, *Spotlight Synthetic Aperture Radar Signal Processing Algorithms,* Artech House Boston. London, 1995, pp423-424.

[9] Wahl,D.E., P.H.Eichel, D.C.Ghiglia, and C.V.Jakowatz, Jr., "Phase Gradient Autofocus—A Robust Tool for High Resolution SAR Phase Correction," *IEEE Transaction on Aerospace and Electronic Systems,* Vol.30, No.3, July 1994, pp.827-83.

[10] Berizzi, and Cosini, G., "Autofocusing of inverse synthetic aperture radar images using contrast optimization," *IEEE Trans AES.* Vol.32, No.3, July 1996, pp.1185-1191.

[11] Wei Ye, Tat Soon Yeo, Zheng Bao,"Weighted least-squares estimation of phase errors for SAR/ISAR autofocus," *IEEE Transaction on Geoscience and Remote Sensing*, Vol.37, No.5. 1999.

[12] Li, Xi, Liu Guosui, Jinlin Ni, "Autofocusing of ISAR Images Based on Entropy Minimization," *IEEE Trans. AES*, Vol.35, No.4, pp.1240-1251, 1999.

[13] Zheng Bao, Changyin Sun, Mengdao Xing, "Time-frequency approaches to ISAR imaging of maneuvering targets and their limitations," *IEEE Trans. AES*, Vol.37, No.3, pp.1091 -1099, Jul 2001.

[14] Genyuan wang, Zheng Bao and Xiaobing Sun, "Inverse synthetic aperture radar imaging of nonuniformly rotating targets," *Optical Engineering*, Vol.35,No.10, Oct. 1996, pp.3007-3011

[15] Trintinalia, L.C.; Hao Ling, "Joint time-frequency ISAR using adaptive processing," *IEEE Transactions on Antennas and Propagation*, Vol.45, No.2, Feb. 1997, pp.221 –227.

[16] V.C.Chen, S.Qian, "Joint time-frequency analysis for radar range Doppler imaging," *IEEE Transaction on Aerospace and Electronic System*, Vol.34, No.2, 1998, pp486-499.

[17] Bao Zheng, Wang Genyuan, Luo Lin, "Inverse Synthetic Aperture Radar Imaging of Maneuvering Targets," *Optical Engineering*, Vol.37, No.5, pp1582-1588, May 1998.

[18] Genyuan Wang, Zheng Bao, "Inverse synthetic aperture radar imaging of maneuvering targets based on chirplet decomposition," *Optical Engineering*, Vol38, No.9, September 1999.

[19] Zheng-She Liu; Renbiao Wu; Jian Li, "Complex ISAR imaging of maneuvering targets via the Capon estimator," *IEEE Transactions on Signal Processing*, Vol.47, No.5, May 1999, pp.1262 –1271.

[20] Berizzi, F.; Mese, E.D.; Diani, M.; Martorella, M., "High-resolution ISAR imaging of maneuvering targets by means of the range instantaneous Doppler technique: modeling and performance analysis," *IEEE Transactions on Image Processing*, Vol.10, No.12, Dec.2001, pp.1880 –1890.

[21] Soumekh, M., *Fourier array imaging,* Englewood Cliffs, NJ: Prentice- Hall, 1994, ch.5.

[22] R.P.Perry, R.C.Dipietro, R.L.Fante., "SAR Imaging of Moving Targets," *IEEE Trans. AES*, Vol.35, No.1, pp.188-199, 1999.

[23] Robert.C. DiPietro, Ronald L. Fante, Richard P. Perry., "Multi-Resolution FOPEN SAR Image Formation," *Part of the SPIE Conference on Algorithms for Synthetic Aperture Radar Imagery VI*, SPIE Vol. 3721, pp58-67.

[24] Chen, V.C., Lipps, R., "ISAR imaging of small craft with roll, pitch and yaw analysis," *Radar Conference, 2000.* The Record of the IEEE 2000 International, 2000. Page(s): 493 –498.

[25] Yuanxun Wang, Hao Ling, "A frequency-aspect extrapolation algorithm for ISAR image simulation based on two-dimensional ESPRIT," *IEEE Transactions on Geoscience and Remote Sensing*, Vol.38, No.4, Part: 1 , July 2000, pp. 1743 –1748.

[26] Xiang-Gen Xia, Genyuan Wang, Chen, V.C, "Quantitative SNR analysis for ISAR imaging using joint time-frequency analysis-Short time Fourier transform," *IEEE Transactions on Aerospace and Electronic Systems*, Vol.38, No.2, April 2002, pp.649 - 659.

[27] Qun Zhang, Tat Soon Yeo, Du, G., "ISAR imaging in

strong ground clutter using a new stepped-frequency signal format," *IEEE Transactions on Geoscience and Remote Sensing*, Volume: 41 Issue: 5 , May 2003, Page(s): 948 –952

[28] J. Li, R. Wu, and V.C. Chen, "Robust autofocus algorithm for ISAR imaging of moving targets," *IEEE Transactions on Aerospace and Electronic Systems*, Vol. 37, No. 3, pp. 1056-1069, July 2001.

[29] D.L. Wehner, *High Resolution Radar*, Norwood, MA:Artech House 1987.

BIOGRAPHY

Xing Mengdao was born in Zhejiang, China, in 1975. He

received the B.S and Ph.D in 1997 and 2002, respectively, from Xidian University. Now he is an associate professor in Key Laboratory for Radar Signal Processing (RSP) of Xidian University. His research interests are radar imaging, target recognition and over the horizon radar (OTHR) signal processing.

Lan Jinqiao was born in Guangxi, China, in 1978. She

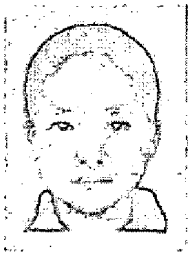

received the B.S in 2001 from Xidian University. Now she is master of Xidian University. Her research interests are radar imaging, system simulation and radar signal processing.

Bao Zheng was born in Jiangsu, China in 1927. He

graduated from the Communication Engineering Institute of China in 1953. Currently, he is a professor at Xidian University and a member of the Chinese Academy of Sciences. He has authored or co-authored 6 books and published over 300 papers. Now, his research fields are space-time adaptive processing (STAP), radar imaging (SAR/ISAR), automatic target recognition (ATR), over-the-horizon radar (OTHR) signal processing, passive coherent location (PCL).

Liao Guisheng was born in Guangxi, China, in 1975. He

received the M.S and Ph.D in 1990 and 1992, respectively, from Xidian University. Now he is a professor in Key Laboratory for Radar Signal Processing (RSP) of Xidian University. His research interests are array signal processing, space-time adaptive proce-ssing (STAP), communication signal processing and so on.